ELSEVIER

Polymer 43 (2002) 1249–1258

polymer

www.elsevier.com/locate/polymer

Influence of ethoxylate chain length for synperonic NPX surfactants on the film formation behaviour of methylmethacrylate–2-ethylhexyl acrylate copolymer latexes: II. A dielectric investigation

Lynda A. Cannon, Richard A. Pethrick*

Department of Pure and Applied Chemistry, University of Strathclyde, Thomas Graham Building, 295 Cathedral Street, Glasgow G1 1X1, UK

Received 25 June 2001; received in revised form 13 August 2001; accepted 2 October 2001

Abstract

A real time dielectric relaxation investigation covering the frequency range from 10^{-2} to $\sim 10^{5}$ Hz, on the film forming process in methylmethacrylate–2-ethylhexyl acrylate latex copolymers stabilised with nonylphenol ethoxylate is presented. The three systems investigated have essentially identical latex compositions and the only difference between these materials is the length of the ethoxylate chain in the nonylphenol ethoxylate stabiliser. The dielectric relaxation measurements allow changes in the dipolar nature of the medium to be monitored as the process of film formation and coalescence occur. Combining the dielectric data with other observations of the coalescence process reported in part 1 has allowed identification of various stages in the film formation process. It is evident that the formation of a microcrystalline phase between the emulsion particles by the longer chain ethoxylate molecules, inhibits the coalescence process. Moreover, the stabiliser can also be seen to play a role in determining the dynamics of the molecules in the latex and a critical role in the overall coalescence process. A schematic model describing the various stages of coalescence is presented. © 2001 Elsevier Science Ltd. All rights reserved.

Keywords: Dielectric relaxation; Acrylic emulsions; Film formation

1. Introduction

In the previous paper [1], a comparison of the film forming characteristics of methylmethacrylate–2-ethylhexyl acrylate latex copolymers stabilised with nonylphenol ethoxylate molecules of varying chain lengths was presented. Using a combination of dynamic mechanical analysis (DMA), minimum film formation temperature (MFFT) measurements, particle size analysis, differential scanning calorimetry (DSC) and atomic force microscopy (AFM), the complexity of the mechanism involved in coalescence in these systems was explored. For the stabiliser with a chain length of 20, coalescence is observed at room temperature; whereas for the longer chain lengths, 30 and 40, coalescence only occurs if the films are raised above 315 K. For the longer chain stabilisers, the effect of stabiliser–stabiliser interaction inhibits the coalescence process and the DSC data indicates the occurrence of crystalline phase structure in the films. In this paper, the application of dielectric methods to study the film formation process are described.

2. Experimental

2.1. Materials—latex preparation

Three methyl methacrylate (MMA)/2-ethylhexyl acrylate (EHA) copolymers were prepared, using the method described previously [2]. The total monomer content was 50 wt% and monomer feed was 34.08 g MMA and 15.89 g EHA. The aqueous phase was buffered with sodium bicarbonate and the polymerisation initiated with potassium persulphate and a second seed of sodium metabisulphite was added half way through the polymerisation. The characteristics of the latex have been presented previously [1] and are summarised in Table 1.

2.2. Latex film characterisation

The latex films were characterised using the following techniques.

* Corresponding author. Tel.: +44-141-548-2260; fax: +44-141-548-4822.

E-mail address: r.a.pethrick@strath.ac.uk (R.A. Pethrick).

0032-3861/02/$ - see front matter © 2001 Elsevier Science Ltd. All rights reserved.
PII: S0032-3861(01)00684-X

Table 1
The characteristic of the latex polymers

Latex-code	% Non-volatiles	MFFT (K)	Mean particle size (nm)	T_g (K), DSC	M_w	M_n
CoME-NP20	39.4	314	221	300	938,000	199,000
CoME-NP30	37.7	316	214	308	1,130,000	230,000
CoME-NP40	39.4	319	219	313	995,000	221,000

2.2.1. Stage one of film formation

The first stage of film formation is defined as the transformation of liquid emulsion into a solid film and was followed by:

Conductance measurements. The conductance of a thin film of the emulsion deposited on a patterned electrode was measured using a 1286 electrochemical interface connected to a BBC computer. The patterned electrode was made from positive resist coated double sided copper clad board using photolithography. A volume of 1 ml of latex was applied to the electrode using a draw down bar which produced a film of 0.1 mm thickness. An applied voltage of 0.01 V was used for the measurements of the conductivity and the resistance between electrode elements was initially observe to be 100 Ω. Measurements were performed at a time interval of 30 s. Dissolved ions in the emulsion gives the latex dispersion a high initial conductivity. As the latex dries, the loss of water causes the ion concentration and conductivity to increase. Further drying leads to particle–particle contact with the creation of a channel structure throughout the 'film'. Further evaporation will close these channels, leaving isolated voids within the film. These voids, may in the initial stage, contain water that will resemble isolated pockets of a salt solution dispersed in an insulating matrix.

2.2.2. Stage two of film formation—the maturation of latex films

When the latex film was macroscopically dry, it was possible to use:

Dielectric spectroscopy. Analysis of the dielectric properties was carried out over the range 10^{-3}–6×10^5 Hz and a temperature range from 270 to 355 K [3]. Electrodes were constructed by lithography on copper clad epoxy resin substrates (Table 1).

The latexes have identical monomer compositions, the difference being the surfactant system used in the polymerisation. As in the previous paper, the designation indicates the length of the ethoxylate chain. As the length of the ethoxylate chain increases, the T_g and MFFT are also observed to increase.

3. Results and discussion

3.1. Conductimetric analysis

The conductance–time profiles for coME-NP20, coME-NP30 and coME-NP40, Fig. 1, show a gradual decline in the conductance with time reflecting slowing down of ion movement. The profile for coME-NP30 indicates a slower drying process than observed in either coME-NP20 or coME-NP40. In the previous paper [1], a study of the change in mechanical properties of a coated braid was used to explore the drying behaviour of the latex dispersions. Below the MMFT, the individual latex particles will firstly come into intimate contact and then a slower rate of evaporation is observed associated with loss of water via the capillaries, which are formed by the touching particles. Above the MFFT, the coalescence of the latex particles occurs at the same time as the evaporation and there is no distinction between these processes. The conductivity measurements reflect the mobility of ions in the aqueous phase and are sensitive to the structure formed as the latex particles attempt to coalesce. In the case of coME-NP20 and coME-NP40, a sharp drop is observed initially in the conductivity, whereas in the case of coME-NP30 the drop is less marked. In the case of coME-NP20, the latex particles will be able to undergo coalescence at room temperature once they come in contact. The initial drop may be interpreted as being purely a reflection of the loss of water from the system. In the case of the coME-NP40, the MFFT is above room temperature and coalescence will be inhibited with the result that channels will remain during drying between the particles. In the case of coME-NP30, the slowing down of the drying process indicates that mobility of ions is retained in these films longer than in the other systems and suggests that the longer ethoxylate chain is able to inhibit the loss of water in this system. The differences in profiles are therefore reflecting both the rate of

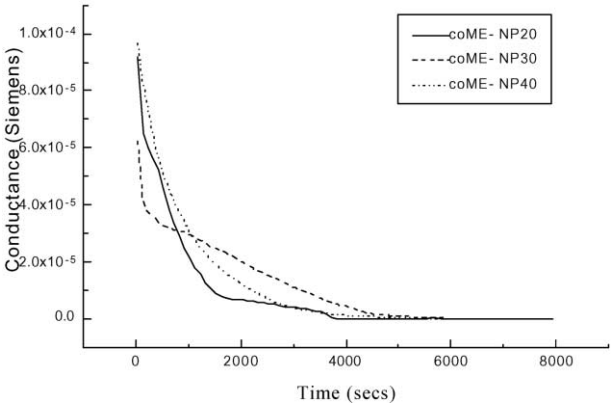

Fig. 1. Conductance–time profile for coME-NPX latexes.

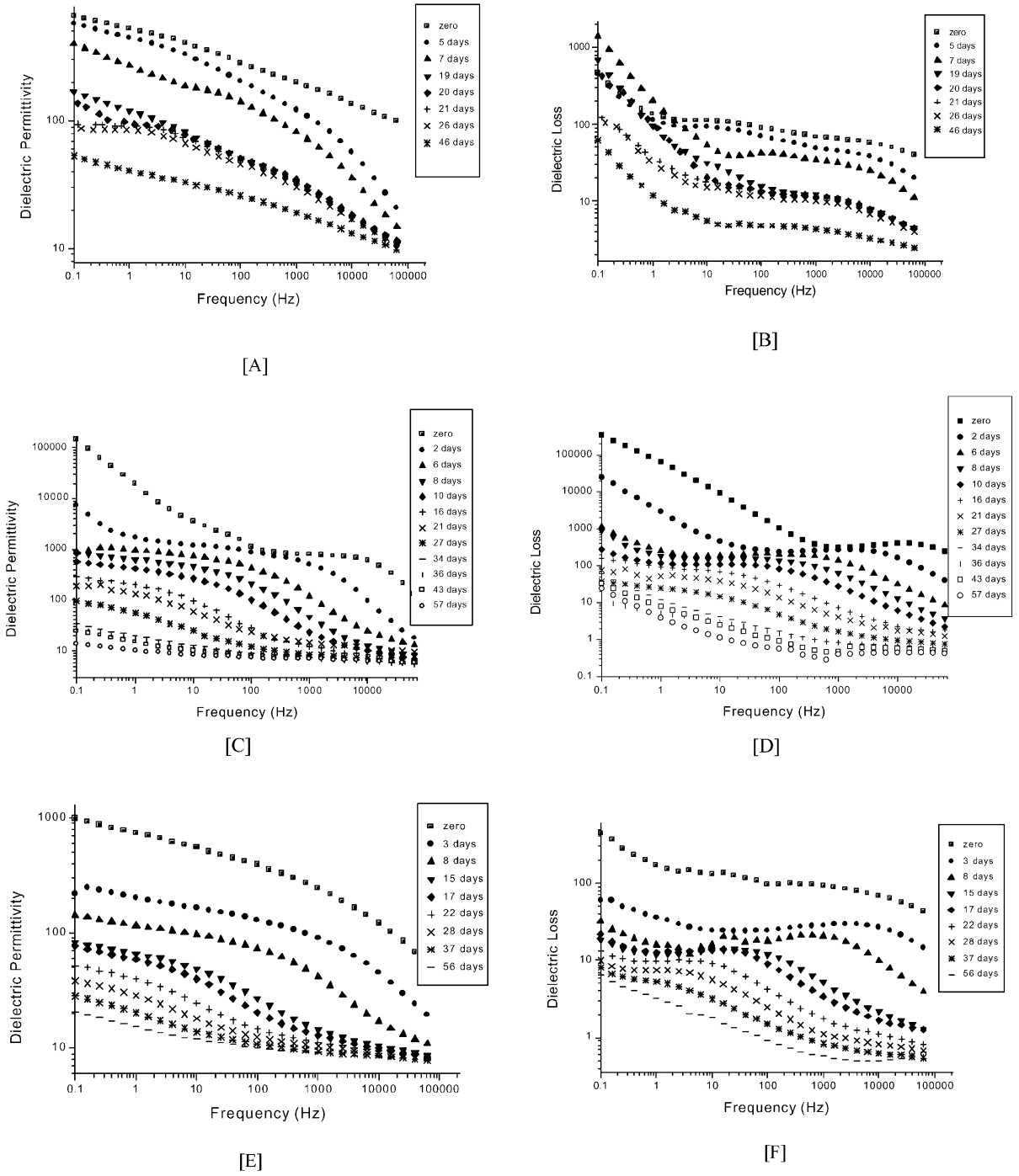

Fig. 2. Change in dielectric permittivity (A) and dielectric loss (B) for coME-NP20; change in dielectric permittivity (C) and dielectric loss (D) for coME-NP30; change in dielectric permittivity (E) and dielectric loss (F) for coME-NP40.

water evaporation and the ability for latex particles to undergo distortion.

3.2. Dielectric spectroscopy under ambient conditions

Analysis of the dielectric spectra were collected over the frequency range 10^{-1}–6×10^{5} Hz at room temperature for films selected at various stages of ageing over 46 day period, Fig. 2. The films were touch-dry at the beginning of these measurements. All the samples investigated exhibited marked changes in their dielectric behaviour over the period of observation. The initial magnitude of the permittivity increment observed is an order of magnitude larger than that observed for a typical dipole relaxation process. The observed dielectric behaviour is associated with a combination of conduction and Maxwell Wagner Sillers (MWS)

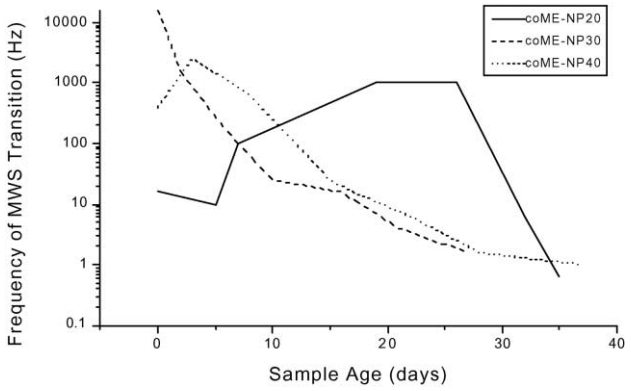

Fig. 3. Plot of the change in f_{MWS} with ageing time for coME-NPX latexes.

effects. The channels which are continuous through the film can sustain d.c. conductivity and will contribute to the loss but not to the permittivity. The large permittivity and the corresponding loss are attributed to a combination of blocking electrode and MWS process. The blocking of ionic mobility either at electrodes or at internal interfaces within the films will lead to the observation of MWS type processes [4–8], Fig. 2. Channels that do not lead to the electrode surface will also inhibit mobility and give rise to MWS phenomenon [4–8].

The dielectric increment $\Delta\varepsilon$, associated with the MWS process, has the form

$$\Delta\varepsilon = \varepsilon_s - \varepsilon_\infty = (v/A)\varepsilon_m \quad (1)$$

where ε_s and ε_∞ are the low and high frequency limiting values of the dielectric permittivity, respectively, v is the volume fraction of the conducting inclusion, A is the depolarisation factor along the axis of the applied electric field and ε_m is the permittivity of the insulating matrix. The location of the process on the frequency axis is defined in terms of its characteristic relaxation time τ which has the form

$$\tau = (\varepsilon_m \varepsilon_0 / A\sigma) \quad (2)$$

where σ is the conductivity of the inclusion and ε_0 is the

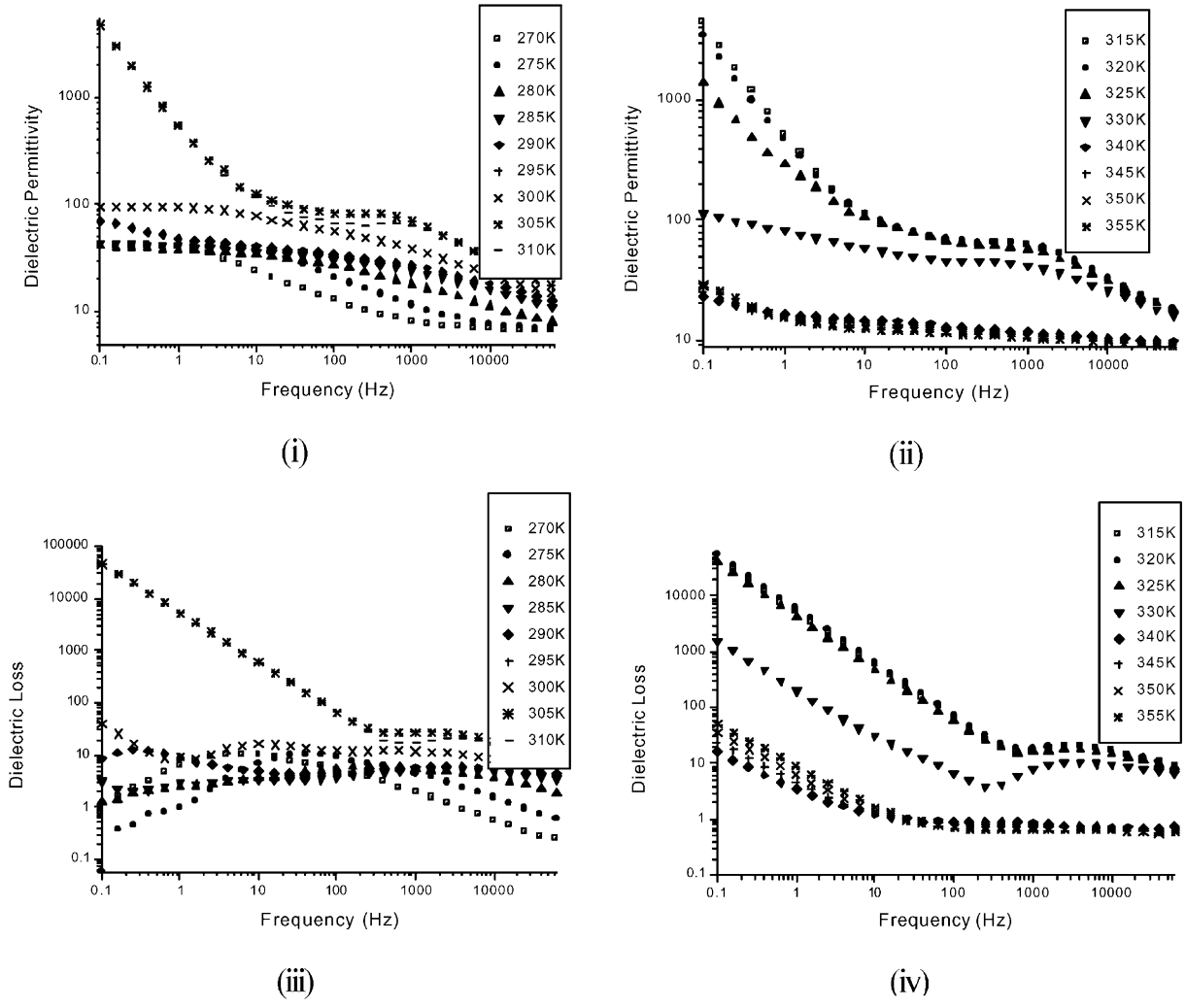

Fig. 4. Dielectric permittivity, (i) and (ii); dielectric loss (iii) and (iv) for an unaged sample of coME-NP20

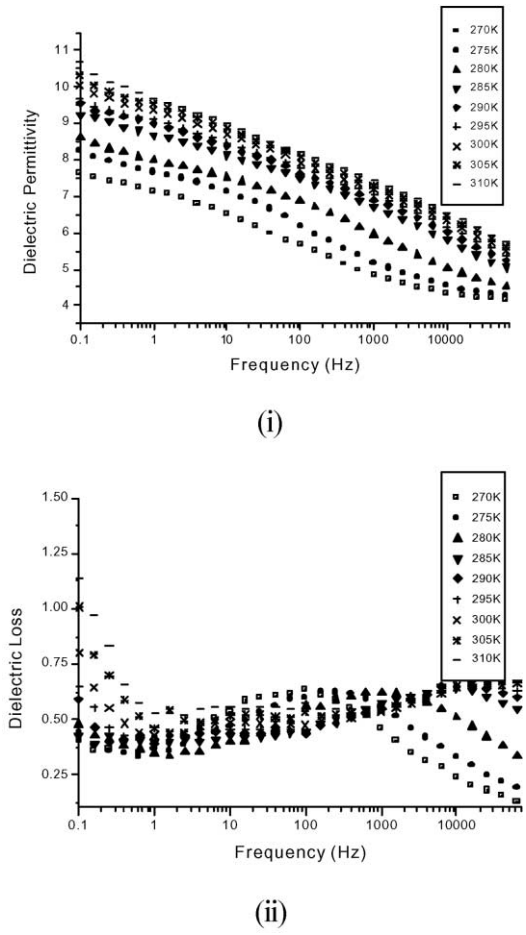

Fig. 5. Dielectric permittivity, (i) and dielectric loss (ii) for a sample of coME-NP20 aged for 47 days.

permittivity of free space. Exact solutions have been obtained for various forms of the occlusions. It may be assumed that the channels formed in the film will have a structure which approximates to a prolate spheroid ($a > b$) where a and b are the length and breadth of the spheroid in the direction of the field axis, respectively, and A has the form [6–8]

$$A = \frac{-1}{(a/b)^2 - 1} + \frac{(a/b)}{[(a/b)^2 - 1]^{3/2}} \ln\{(a/b) + [(a/b)^2 - 1]^{1/2}\} \quad (3)$$

The above equations need to be combined with the Debye equations to allow prediction of the frequency dependence of the dielectric response

$$\varepsilon'(\omega) = \varepsilon_\infty + \frac{\varepsilon_s - \varepsilon_\infty}{(1 + \omega^2\tau^2)} \quad (4)$$

and

$$\varepsilon''(\omega) = \frac{(\varepsilon_s - \varepsilon_\infty)\omega\tau}{(1 + \omega^2\tau^2)} \quad (5)$$

A decrease in the conductivity would shift the relaxation frequency associated with the MWS process to lower frequency, whereas a shortening of the conduction path would lead to an increase in the relaxation frequency. The characteristic relaxation frequency in all three systems initially shifted to lower frequency as the film dried. Inspection of Eq. (2) indicates that increasing the relaxation time implies either a decrease in conductivity or the A factor. The A factor is determined by the length to breadth ratio of the conducting channel. The breadth of the channel is likely to stay approximately constant as it is defined by the close packed structure of the latex particles. The apparent increase in the relaxation frequency for coME-NP20 may be explained in terms of either an increase in conductivity of the channel as the water evaporates or an increase in the A factor. The latter implies that the channels are becoming shorter and would be consistent with coalescence and a decrease in the length of the channels. An alternative explanation that cannot be excluded is that the evaporation of water is leading to an increased conductivity in the channels as the films dry. The bulk conductivity will be dropping as described earlier, but this does not exclude the reverse occurring within the channels although this would appear rather unlikely. Beyond 30 days, the conductivity drops as the loose water in the channels become dominant and the relation frequency is lowered. The relaxation is very broad and it is difficult to assign an unambiguous interpretation of the trends observed. Shortening of the channels will lead to an increase in the frequency that is not observed in practice.

The trend in f_{MWS} is different for coME-NP30 and coME-NP40 from that observed for coME-NP20 (Fig. 3). In the coME-NP30 and come-NP40 systems, the decrease in f_{MWS}, implies that the conductivity is decreasing faster than the shortening of the conducting channel path length. These particular systems cannot undergo coalescence at these temperatures and the ethoxylate chains once they overlap can start to crystallise and assist in reduction of the ionic mobility. The ethoxylate crystallites will increase in the percolation path by which the water molecules and ions moved between the bulk and the surface of the film and will influence conductivity and mobility of the ions in the matrix. A decrease in the conductivity will lead to a lowering of the frequency of the MWS relaxation process, whereas shortening of the channels would lead to an increase in the relaxation frequency.

Crystallite formation will effectively decrease the conductivity and this mechanism exists in the case of the coME-NP30 and coME-NP40 systems. Increasing the size of crystalline domain will have the same effect as decreasing the MWS path length and will shift f_{MWS} to lower frequencies.

3.3. Dielectric thermal analysis of film formation in coME-NPX

Dielectric measurements were performed over a frequency range of 10^{-1}–6×10^5 Hz and a temperature

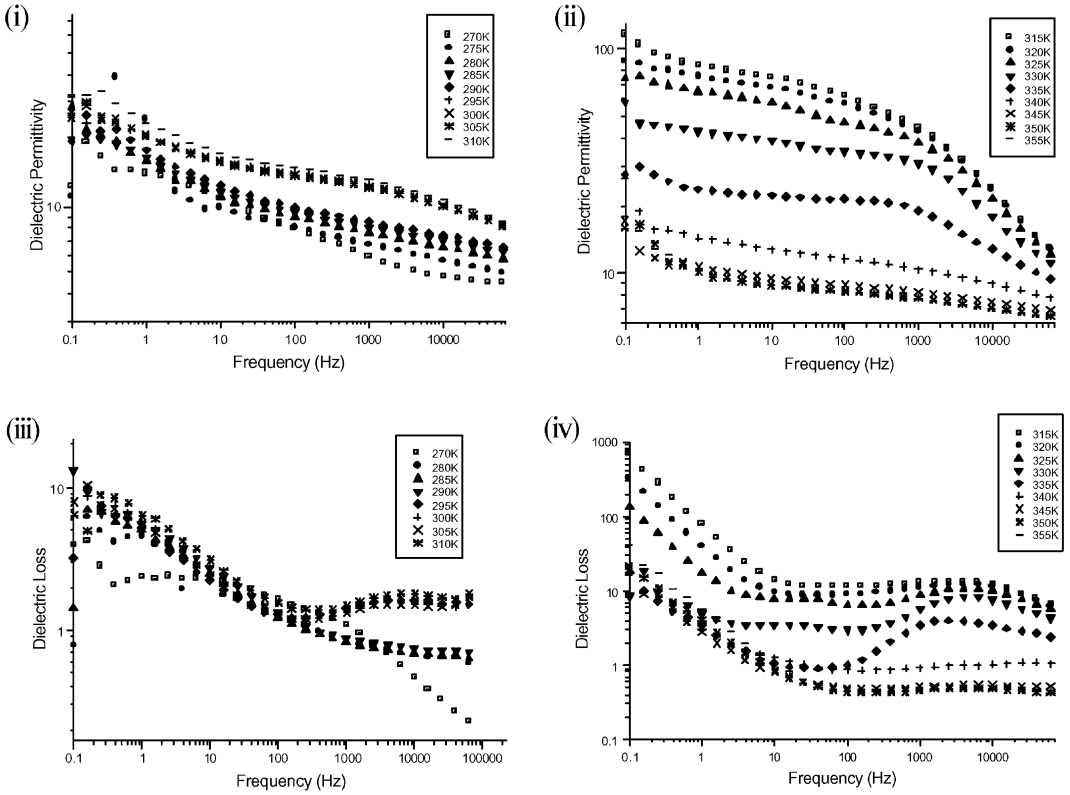

Fig. 6. Dielectric permittivity, (i) and (ii); dielectric loss (iii) and (iv) for a sample of coME-NP30 unaged.

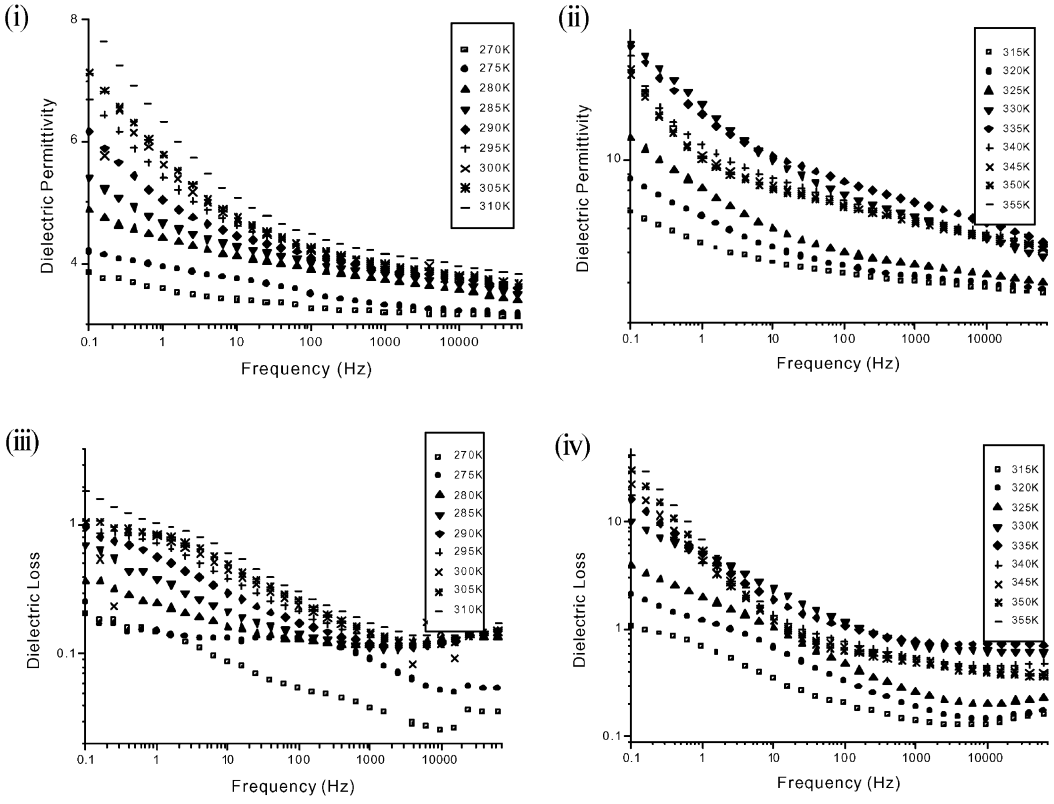

Fig. 7. Dielectric permittivity, (i) and (ii); dielectric loss (iii) and (iv) for a sample of coME-NP30 aged for 36 days.

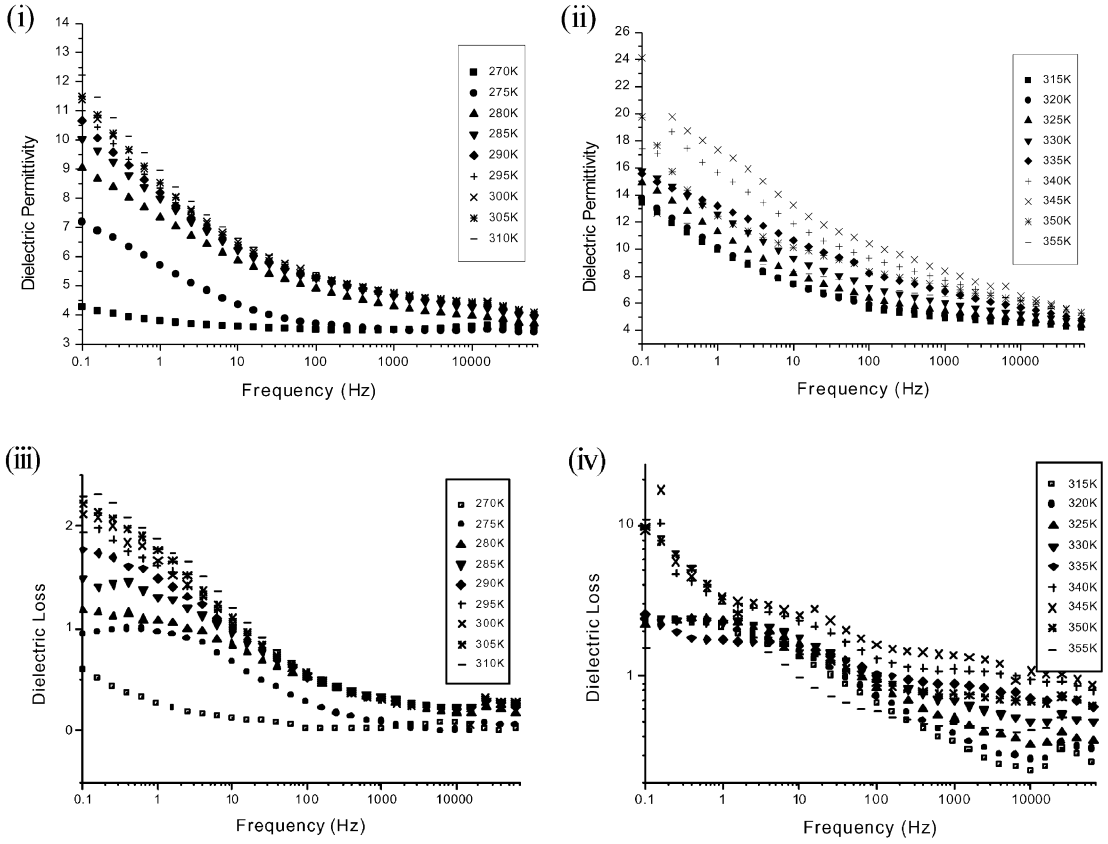

Fig. 8. Dielectric permittivity, (i) and (ii); dielectric loss (iii) and (iv) for a sample of coME-NP40 unaged.

range of 270–355 K at an interval of 5 K, the temperature being equilibrated for 30 min before measurements were taken [15]. This study was carried out in an attempt to determine more precisely the nature of the relaxation process discussed earlier. The dielectric permittivity and loss data for the three latexes were measured for an unaged sample, after 4, 8, 14, 28, 34 and 47 days and representative data for the unaged and aged samples are presented in Figs. 4–9. A complete set of dielectric measurements is available elsewhere [9]. The dielectric data can be interpreted in terms of four processes. Firstly, a d.c. conductivity contribution resulting from retained water in the latex films; secondly, blocking electrode effects associated with slow discharge of charge at the electrodes; thirdly, the MWS effects from inclusions formed by channels closing or being blocked by crystallite formation; and fourthly, dipolar relaxation due to motion of the ester groups of the acrylic polymer chains.

Conductivity contributes to the dielectric loss but not to the permittivity and disappears after 14 days for coME-NP20; after six days coME-NP30 and 0 day for coME-NP40. The trend previously seen in the mechanical measurements [1], in which proficient loss of water from the coME-NP40 latex is also seen in the dielectric data. AFM observations of the coME-NP40 films also showed that the packing was less perfect and there was a higher void content visible. The MWS and blocking electrode contributions give rise to large values of the permittivity and are associated with the formation of crystalline phases through interaction of ethoxylate chains. A plot of the permittivity at 1 Hz for each sample over the ageing period indicates the reduction in the MWS and blocking electrode contributions with time, Fig. 10. The residual permittivity can be associated with the motion of the dipoles of the acrylic polymer. Loss of inclusions and conducting channels are responsible for the reduction in the amplitude of the MWS process and are associated with the coalescence process. Identification of the temperature at which a decline in the permittivity occurs is a direct indication of coalescence and loss of heterogeneity in the sample. The maximum temperature also provides information on the amount of energy required facilitating coalescence and is therefore related to the degree of compaction and deformation in the sample, Fig. 11.

The magnitude of the dielectric permittivity declines from coME-NP20 to coME-SP40. The difference in permittivity value between the three latex samples can be attributed to the amount of retained water in the sample. As the size of the crystalline domain in the sample increases, the amount of retained water decreases and the permittivity is lowered.

As the samples age, the coalescence temperature of the

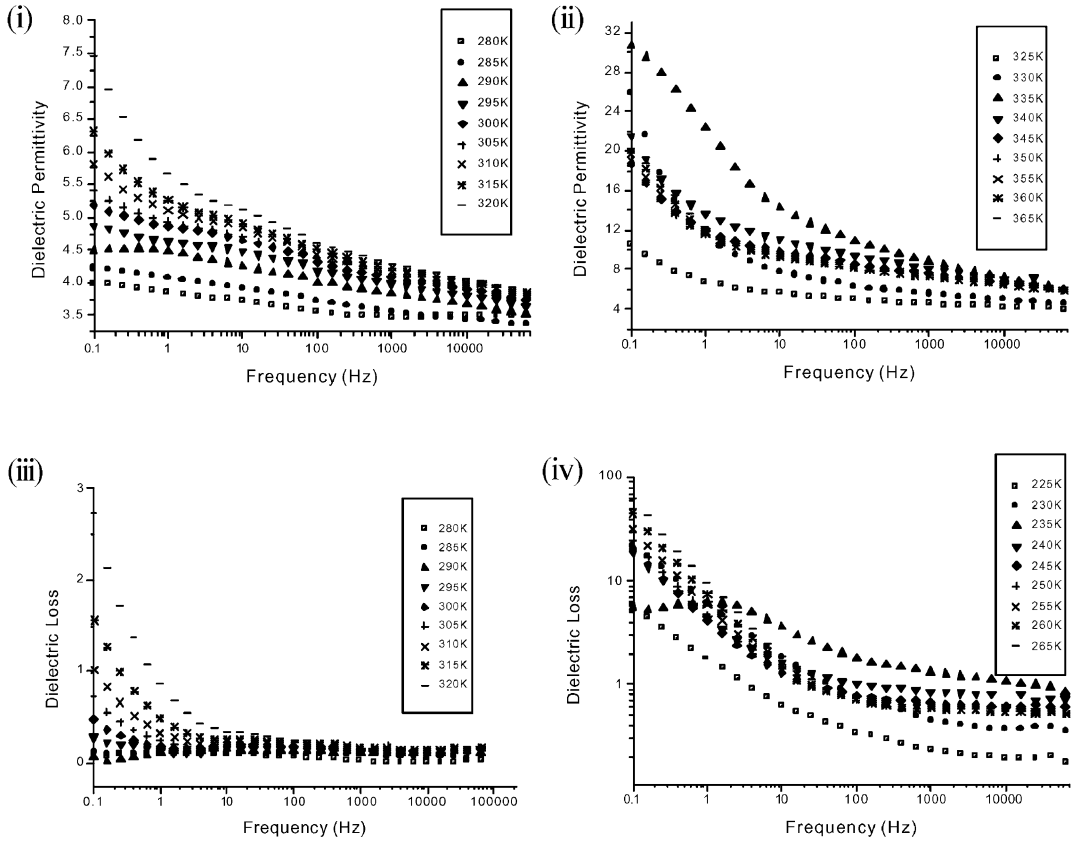

Fig. 9. Dielectric permittivity, (i) and (ii); dielectric loss (iii) and (iv) for a sample of coME-NP40 aged for 53 days.

latexes increases indicating that more energy is required to achieve homogeneity. Initially, water can act as a plasticiser, its loss allows PEG chains to crystallise and inhibit coalescence. As the length of the ethoxylate chain of the surfactant increases in going from coME-NP20 to coME-NP40, the coalescence temperature of the film increases. Since the latexes have similar chemical structures, the variation in T_g can only be attributed to surfactant effects. NPX may be assumed to be a plasticiser and its distribution between the polymer and PEG rich phase will influence the dynamic properties of the material. The formation of crystalline regions in the surfactant rich phase will change the constraints at a local level placed on the motion of the polymer and surfactant chains. As the length of the ethoxylate chain on the surfactant increases, the melting temperature of the segregated PEG region increases and so the amount of energy required to destroy these domains also increases.

In the coalesced films, the dipolar activity becomes dominant and the activation energy for this process is obtained from Arrhenius plots of the relaxation frequency against reciprocal temperature. The activation energies calculated from the dielectric measurements, coME-NP20 was 204 ± 18 kJ mol^{-1} after 0 days; 137 ± 47 kJ mol^{-1} after 4 days; 215 ± 51 kJ mol^{-1} after 14 days; 239 ± 55 kJ mol^{-1} after 28 days; 273 ± 12 kJ mol^{-1} after 47 days The magnitude of the activation energy calculated is comparable to that which would be expected for short range or side chain motions. The variation in the activation energy may in part reflect the effects of loss of water of solvation and is consistent with the higher observed values of the T_g reported in part I [1]. The initial drop in the activation energy between 0 and 4 days is attributed to a combination of effects. In the initial stages of drying of the emulsion, the surfactant molecules form a bridge between neighbouring particles. These surfactant molecules possess polyether groups that will be hydrated and can therefore be hydrogen bonded together. As drying occurs, water will be lost and constraints on the interface will be reduced favouring inter-diffusion of surfactant and acrylic polymer chains located close to the surface layer. This process appears to produce a plasticization of the polymer chains and a consequent reduction in activation energy for dipole rotation. Further loss of moisture and further inter diffusion of stabiliser and acrylic polymer chains reduces the plasticization effect and the activation energy is observed to progressively increase.

Dielectric analysis of the other latexes indicate that the motion of polymer chains is inhibited and it was not possible to calculate an activation energy in coME-NP30 and coME-NP40. The presence of regions of crystallinity between the latex particles will inhibit translation and rotational motion of the polymer chains.

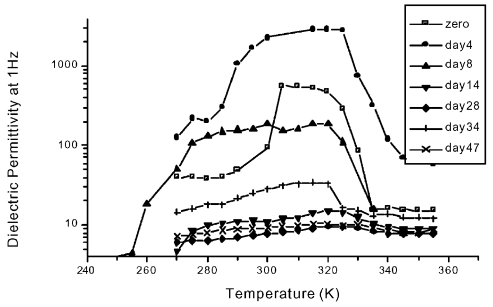

[A]

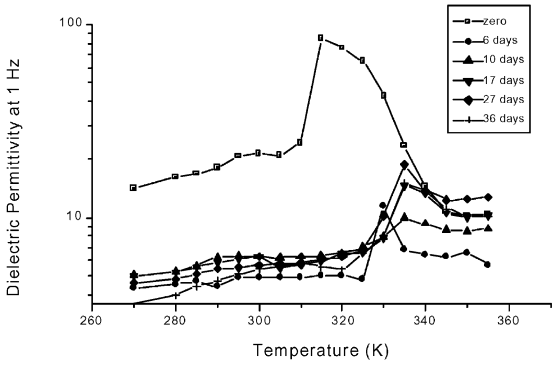

[B]

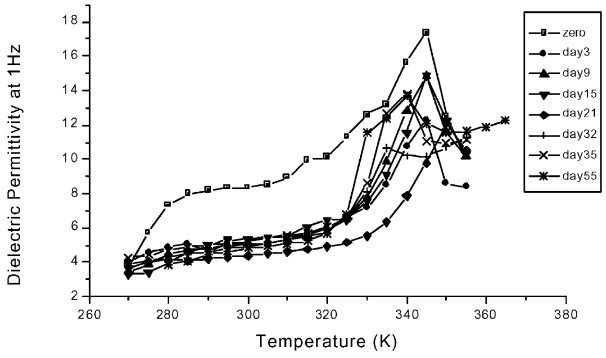

[C]

Fig. 10. Permittivity (1 Hz)–temperature plots for (A) coMe-NP20; (B) coME-NP30; and (C) coME-NP40.

4. Conclusions

A variety of models have been proposed to describe the coalescence process [10–21]. In order to include the observations form this paper, an extension of these models will be presented. The latexes under investigation are identical in monomer composition, only the surfactant is different. The mechanical analysis of the three polymers revealed a two stage-drying profile, and conforms to

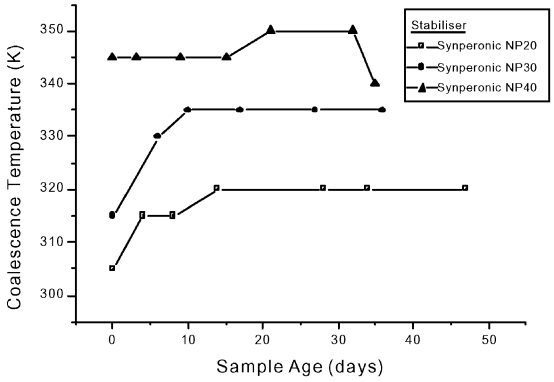

Fig. 11. Variation of the coalescence time.

model 2 of drying. This model defines a point x (the end of stage one) as the point at which evaporation kinetics due to particle close packing. The subsequent kinetics are influenced by particle deformation and are reflected in the change in mechanism once the MFFT has been exceeded. The activation energies and rate constants calculated for stage one of the drying processes indicate that it is essentially and evaporation process. Stage two is influenced by two factors; particle deformation and the formation of crystalline domains in the surfactant rich inter particle phase. Such domains would aid the development of the mechanical integrity of the films, but the level of hydration of the inter particulate domain was also found to be influenced.

Dielectric measurements performed under ambient

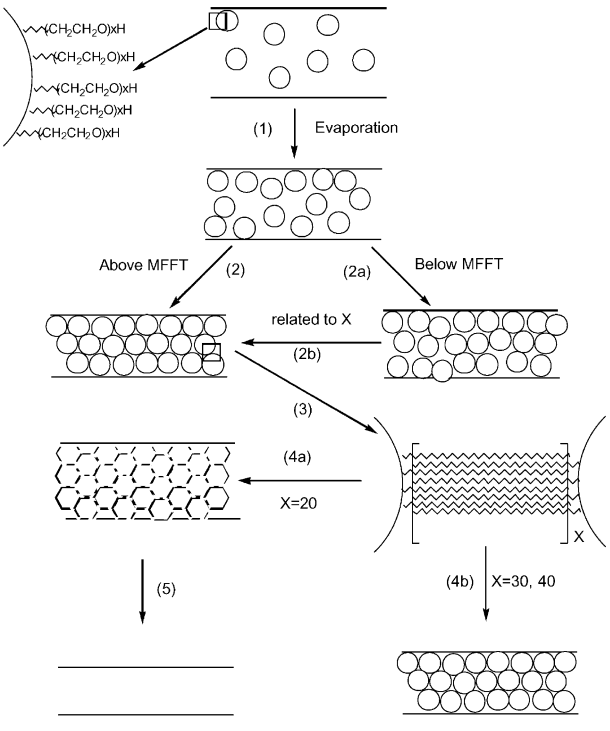

Fig. 12. Model of film formation in latexes stabilised by Synperonic NPX, ($X = 20, 30, 40$).

conditions were used to map the maturation of the latex film. The dielectric spectra obtained showed a decrease in the dielectric permittivity value and a reduction in the conductivity contribution as the samples aged. Analysis of the spectra indicated the existence of an MWS relaxation process in all three systems. Mapping the change of frequency (f_{MWS}) at which the process occurs against time indicated the growth and change in shape and physical properties of inclusions in the film. The data also provides evidence for the presence of crystalline domains in coME-NP30 and coME-NP40 and the absence of such regions in coME-NP20. The data indicates that in the case of coME-NP20 both compaction and deformation can occur during film formation. However, for coME-NP30 and coME-NP40 formation of crystalline domains in the inter particle region reduces the conductivity and there is little evidence for significant article deformation. Here the profile of f_{MWS} indicates a reduction in conductivity only with no compaction or deformation. Such effects would result from the presence of crystalline regions between the latex particles serving as a mechanical barrier to coalescence.

The overall model, Fig. 12, for the film formation process appears to be as follows:

1. Evaporation of water from the latex increases the solids fraction in the dispersion.
2. The latex dried at a temperature above its MFFT has sufficient mobility to allow a dense close packed structure to be creased. Below the MFFT of the latex, evaporation of water continues until a solids volume fraction of ~0.7 is reached, when the rate is observed to change as a consequence of the restraints imposed by particle deformation on the kinetics. The two stage-drying model is a feature of the particle's resistance to deformation. In the case of ethoxylate containing stabilisers, the possibility of crystallisation in the interparticle phase exists and has a profound effect on the overall behaviour.
3. Of the three systems investigated, only coME-NP20 exhibits any evidence of true coalescence of the polymer particles, the process being inhibited in the high molar mass containing materials by the formation of crystalline domains.

Acknowledgements

The support of LAC by EPSRC and ICI in the form of a CASE award is gratefully acknowledged. The interest of Dr David Elliott and Dr David Taylor in the project is also gratefully acknowledged.

References

[1] Cannon LA, Pethrick RA. Polymer 2002;43:1223.
[2] Cannon LA, Pethrick RA. Macromolecules 1999;32:7617.
[3] Hayward D, Mahoubian Jones G, Pethrick RA. J Phys E: Sci Instrum 1984;17:683.
[4] Hedvig P. Dielectric spectroscopy of polymers. Bristol: Adam Hilger, 1977.
[5] North AM, Pethrick RA, Wilson AD. Polymers 1978;19:913.
[6] Van Beek LKH, Booy J, Looyenga H. Appl Sci Res 1965;12:57.
[7] Hayward D, Pethrick RA, Siriwittayakorn T. Macromolecules 1992;25:1480.
[8] Van Beek LKH. Prog Dielectric 1967;7:69.
[9] Cannon L. PhD Thesis, University of Strathclyde, 1998.
[10] Eckersley ST, Rudin A. Film formation in waterbourne coatings. In: Provder T, Winnik MA, Urban MW, editors. ACS Symposium Series, vol. 648. 1996. p. 2.
[11] Niu BJ, Martin LR, Tebelius LK, Urban MW. Film formation in waterbourne coatings. In: Provder T, Winnik MA, Urban MW, editors. ACS Symposium Series, vol. 648. 1996. p. 301.
[12] Keddie JL, Meredith P, Jones RAL, Donald AM. Film formation in waterbourne coatings. In: Provder T, Winnik MA, Urban MW, editors. ACS Symposium Series, vol. 648. 1996. p. 332.
[13] Ming-Da Eu, Ullman R. Film formation in waterbourne coatings. In: Provder T, Winnik MA, Urban MW, editors. ACS Symposium Series, vol. 648. 1996. p. 79.
[14] Winnik MA. Film formation in waterbourne coatings. In: Provder T, Winnik MA, Urban MW, editors. ACS Symposium Series, vol. 648. 1996. p. 51.
[15] Routgh AF, Russel WB. AICHE J 1998;44(9):2088.
[16] Feng JR, Winnik MA. Macromolecules 1997;30(15):4324.
[17] Wang YC, Winnik MA. J Phys Chem 1993;97(11):2507.
[18] Winnik MA, Winnik FM. Advances in chemistry series, vol. 236. Washington, DC: American Chemical Society, 1993 p. 485.
[19] Keddie JL, Meredith P, Jones RAL, Donald AM. Macromolecules 1995;28:2673–82.
[20] Sperry PR, Snyder BS, O'Dowd ML, Lesko PM. Langmuir 1994;10:2619.
[21] Keintz E, Holl Y. Colloids Surf A—Physicochem Engng Aspects 1993;78:255–70.